Fusion of Spectra and Texture in Hyperspectral Imaging for Quantification of Nutritional Content in Alfalfa-Potato Pomace

Wenbin Guo,[a,b,#,*] Tianyu Shi,[a,b,#] Xiaowei Jin,[a,b] and Xuhui Zhang [a,b]

** Corresponding author: wenbingwb2000@sina.com;*
 # Wenbin Guo and Tianyu Shi have contributed equally to this work and share first authorship.

DOI: 10.15376/biores.20.4.10249-10262

GRAPHICAL ABSTRACT

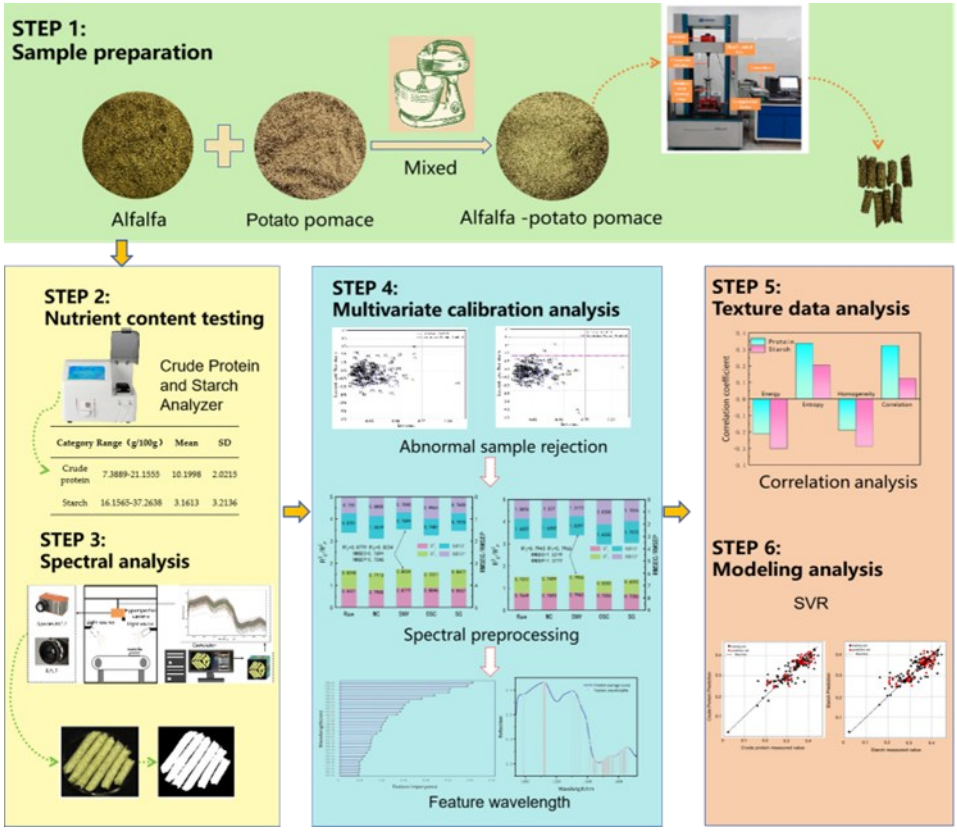

Fusion of Spectra and Texture in Hyperspectral Imaging for Quantification of Nutritional Content in Alfalfa-Potato Pomace

Wenbin Guo,[a,b,#,*] Tianyu Shi,[a,b,#] Xiaowei Jin,[a,b] and Xuhui Zhang [a,b]

Rapid and accurate detection of crude protein and starch content in alfalfa-potato pomace pellets is crucial for improving their processing and enhancing nutritional quality. In this study, hyperspectral images of alfalfa-potato pomace pellets in the near-infrared (NIR) range (900 to 1700 nm) were acquired. A support vector regression (SVR) model was developed by combining various spectral preprocessing methods and effective wavelength selection techniques. Textural features from the surface of the first principal component (PC1) image sample were also extracted using the gray-level co-occurrence matrix (GLCM) and fused with the spectral data, significantly improving the model's prediction accuracy. The results indicated that the SNV-GB-COR-SVR model performed best in predicting crude protein content, with an R^2p of 0.907 and an RMSEP of 0.5548, while the SNV-CARS-ENT-SVR model was most effective in predicting starch content, with an R^2p of 0.7915 and an RMSEP of 1.3970.

DOI: 10.15376/biores.20.4.10249-10262

Keywords: Hyperspectral image technology; Near-infrared spectroscopy; Texture; Gray-level co-occurrence matrix; Crude protein; Starch

Contact information: a: College of Electromechanical Engineering, Inner Mongolia Agricultural University, Hohhot 010018, Inner Mongolia, China; b: Inner Mongolia Engineering Research Center of Intelligent Equipment for the Entire Process of Forage and Feed Production;
** Corresponding author: wenbingwb2000@sina.com;*
 # Wenbin Guo and Tianyu Shi have contributed equally to this work and share first authorship.

INTRODUCTION

With the continuous development of the feed industry and animal husbandry, the nutritional value of pellet feed has gained increasing emphasis. This value not only directly affects the growth and health of animals but also plays a crucial role in the quality of livestock products. Consequently, detecting and enhancing the nutritional value of pellet feed promptly has become a key focus of current research. As important feed resources, alfalfa and potato pomace have attracted significant attention due to their rich nutritional content and economic benefits. Alfalfa is widely used in feed because of its high crude protein content and low neutral detergent fiber (Hadidi *et al*. 2023). Potato pomace, a by-product of starch processing, is also commonly used in livestock feed because of its nutrients, including starch, cellulose, protein, and amino acids (Guo *et al*. 2017). Therefore, mixing alfalfa meal, which is not easily molded, with potato pomace for pellet feed production not only takes advantage of the natural binding effect between these materials to reduce pelleting costs but also addresses issues like nutritional imbalance and low feeding rates caused by using a single type of feed, thereby improving feed quality.

Accurate testing of nutrient content is essential in the process of enhancing the nutritional value of pellet feeds. Taking alfalfa-potato pomace pellets as an example, the crude protein and starch content are key nutritional quality indicators, directly influencing both the nutritional quality of the feed and the growth and development of animals (Rocha *et al*. 2022). However, these key indicators are typically tested using chemical methods, which are complex, time-consuming, and costly. This constraint limits the ability to quickly assess nutrients during the development of high-quality pellet feeds. Therefore, finding a fast, accurate, and stable method for nutritional quality testing, such as through hyperspectral imaging (HSI) and other techniques, has become crucial to optimizing pellet feed processing.

The hyperspectral imaging (HSI) technique, which integrates both spectral and image information, is an advanced and rapid method for nondestructive testing. It has been widely applied in feed quality assessment (Yan *et al*. 2019), particularly for predicting protein content (Fu *et al*. 2017), pH value (Zhang 2023), and moisture content (Yu *et al*. 2023). These studies have demonstrated the feasibility of using HSI to predict crude protein and starch content in pelleted feeds. However, most existing prediction models are based solely on spectral data, which captures only the chemical compositional information of the particles. As a result, the surface microtexture features of the particles and their spatial distribution, which are also important, are not analyzed. Texture features, an important aspect of image spatial information, reflect characteristics of the sample surface, such as fine structure, homogeneity, orientation, and roughness (Yang 2024). These features effectively complement spectral information. Recently, several researchers have highlighted the importance of simultaneously analyzing both HSI spectral and spatial information. Examples include the prediction of palmitic and oleic acid content in lamb (Wang *et al*. 2020), the prediction of the K-value of pork (Cheng *et al*. 2016), the prediction of pH-value in salted meat (Liu *et al*. 2014), and the prediction of volatile saline nitrogen content in cooked beef using texture features and color models (Yang *et al*. 2017). These studies suggest that combining spectral and spatial information from HSI provides a more comprehensive and intuitive analysis compared to traditional methods. The fusion of spectral and texture features through multidimensional analysis is expected to significantly enhance the accuracy and robustness of detecting crude protein and starch content in pellet feed, providing new technical support for the rapid nondestructive testing of feed quality.

The 900 to 1700 nm wavelength range was chosen for this study because it effectively captures absorption features of key chemical groups in feed components. It detects N-H bending and C=O stretching vibrations in proteins, which are essential for predicting protein content (Du *et al*. 2024). Additionally, starch and other sugars show distinct absorption characteristics in this range, aiding in starch estimation. Previous studies have shown that NIR spectroscopy in this range is effective for analyzing crude protein and starch in feed. For example, Tang *et al.* (2004) used hyperspectral methods to estimate the crude protein and crude starch content in rice ears and grains. Rukundo *et al.* (2021) demonstrated that handheld NIR spectrometers (900 to 1700 nm) can accurately predict protein content in animal feed, making them suitable for field use .

The main objective of this study was to utilize the combination of spectral and image texture information to predict the crude protein and starch contents in alfalfa-potato pomace pellet feed. Hyperspectral data of the pellet feed, ranging from 900 to 1700 nm, were collected. The optimal preprocessing method and characteristic wavelength selection were determined by applying four preprocessing methods and two variable selection tools. Texture information of the pellet feed was extracted using the gray-level co-occurrence

matrix. An SVR prediction model was then established, based on both the spectral data and the fusion of spectral and texture information, to predict the crude protein and starch content in the pellet feed.

It was hypothesized that the textural features of pellet feed are crucial because key nutrients, such as crude protein and starch, may be unevenly distributed within the pellet. Nutrients could concentrate in specific areas, influenced by the pellet's shape and surface structure. For example, surface roughness or homogeneity may correlate with nutrient density in particular regions. By combining textural and spectral data, we can enhance the understanding and accuracy of crude protein and starch content predictions, thereby improving the robustness of feed quality models.

EXPERIMENTAL

Sample Preparation

The test samples used in this study were pellet feeds compressed and molded from alfalfa meal mixed with potato pomace, produced in Hohhot, Inner Mongolia. The initial moisture contents of the alfalfa meal and potato pomace were 15% and 60%, respectively. After pressing and molding, the resulting alfalfa-potato pomace pellet feeds were randomly selected and weighed, with individual samples weighing approximately 70 g and having a pellet diameter of 8 mm. A total of 201 samples were numbered, placed in self-sealing bags (14 cm × 20 cm), and stored in a refrigerator at about 8 °C.

Nutrient Content Testing

The determination of crude protein content in feed was carried out using the Kjeldahl method, following the GB/T 6432 (2018) standard (Huang *et al*. 2021). The crude protein content was calculated using the following formula,

$$crude\ protein\ content(\%) = \frac{(V_1 - V_0) \times C \times M \times p}{m} \times 100 \quad (1)$$

where V_1 is the volume of standard acid solution consumed in the titration of the sample(mL), V_0 is the volume of standard acid solution consumed in the titration of the blank(mL), C is the concentration of the standard acid solution(mol/L), M is the molar mass of nitrogen(g/mol), p is the conversion factor of protein, and m is the mass of the sample(g).

The starch content was determined according to the GB/T 15683 (2008) standard using the following formula,

$$starch\ content\ (\%) = \frac{C \times V \times p}{m} \times 100 \quad (2)$$

where C is the concentration of reducing sugar in the sample solution(g/L), V is the total volume of the sample extract(mL), p is the conversion factor for the conversion of starch to glucose, and m is the sample mass(g).

Hyperspectral Data Acquisition and Information Extraction

Hyperspectral image acquisition

Hyperspectral data acquisition of pellet feed was performed using a Specim FX17 hyperspectral imaging system (Specim, Oulu, Finland). The system consists of a Specim FX17 hyperspectral camera, a 150 W halogen lamp, a sample stage, and a computer, as shown in Fig. 1. The camera captures spectral data from 900 to 1700 nm across 224 bands. The light sources are positioned on both sides of the sample stage at a height of 50 cm.

Before taking measurements, the instrument underwent a 20-minute warm-up period to ensure the light source was stable. It was then calibrated using a standard whiteboard. Each pellet feed sample was measured three times independently, and the average of these measurements was recorded. After the spectral data was collected, it was saved in a designated folder on the computer and calibrated using the Lumo Scanner software by Specim to guarantee the precision and reliability of further analyses.

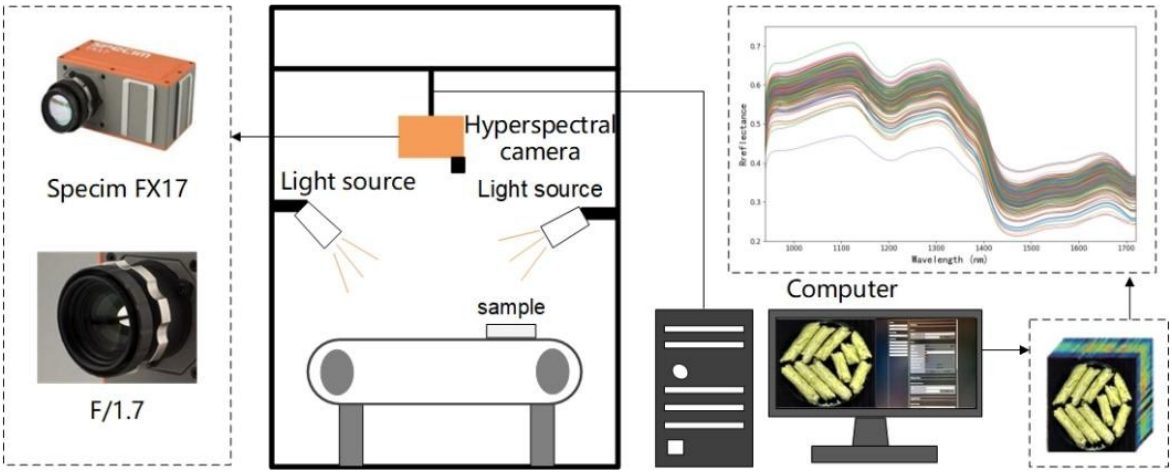

Fig. 1. The hyperspectral imaging system

Spectral information extraction

Spectral data with significant features were extracted using Python 3.11 software. The pixel values of the pseudo-color images were clustered and segmented using the K-means algorithm, and the resulting segmentation map was visualized. Cluster labels were manually selected to create the mask map (ROI), which was used to extract the spectral data and calculate the average reflectance for each band. The extraction results are shown in Fig. 2, where Fig. 2a shows the original spectral image, and Fig. 2b highlights the portion of the white area containing the alfalfa-potato pomace pellet sample.

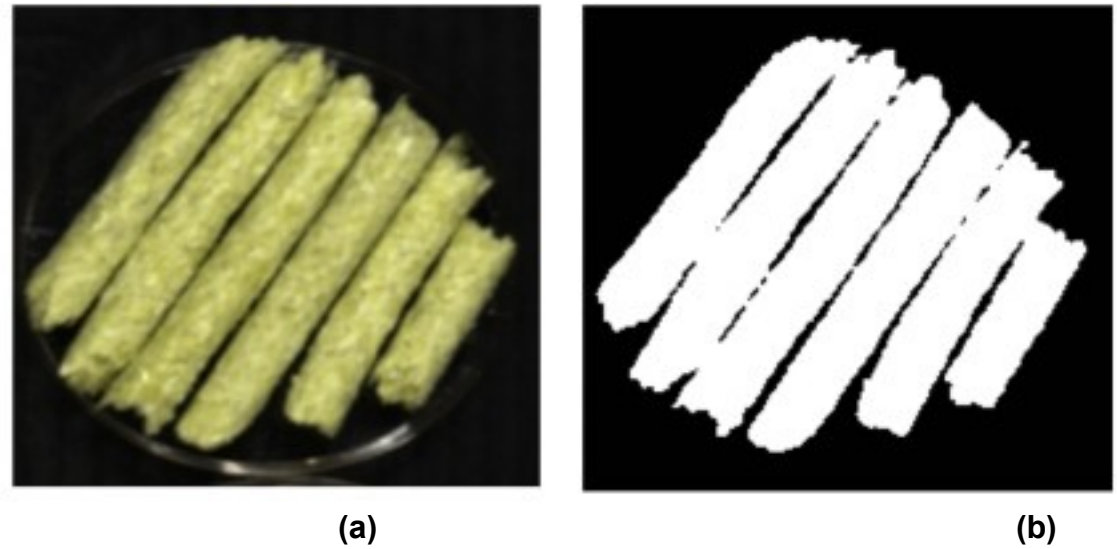

(a) **(b)**

Fig. 2. Selection of Alfalfa-Potato Pomace Pellet Feed Area. (a) Original spectrogram; (b) Algorithm selected region

Data Preprocessing

Abnormal sample rejection

During the process of spectral data collection and nutrient testing, abnormal values may arise due to instrumental interferences, which can significantly impact the performance of subsequent prediction models. Therefore, in this study, a combination of leverage and studentized residuals was used to detect abnormal samples (Xie 2013).

The results of abnormal sample detection for crude protein and starch content in alfalfa-potato pomace pellets are shown in Fig. 3. The crude protein abnormal value detection results in Fig. 3a indicate that both the leverage value and the student residuals of sample No. 16 exceeded the set threshold range, leading to its identification as an abnormal sample. Similarly, the starch abnormal value detection results in Fig. 3b show that samples No. 16 and No. 18 were recognized as abnormal. The statistical results for each nutrient content, after rejecting the abnormal samples, are presented in Table 1.

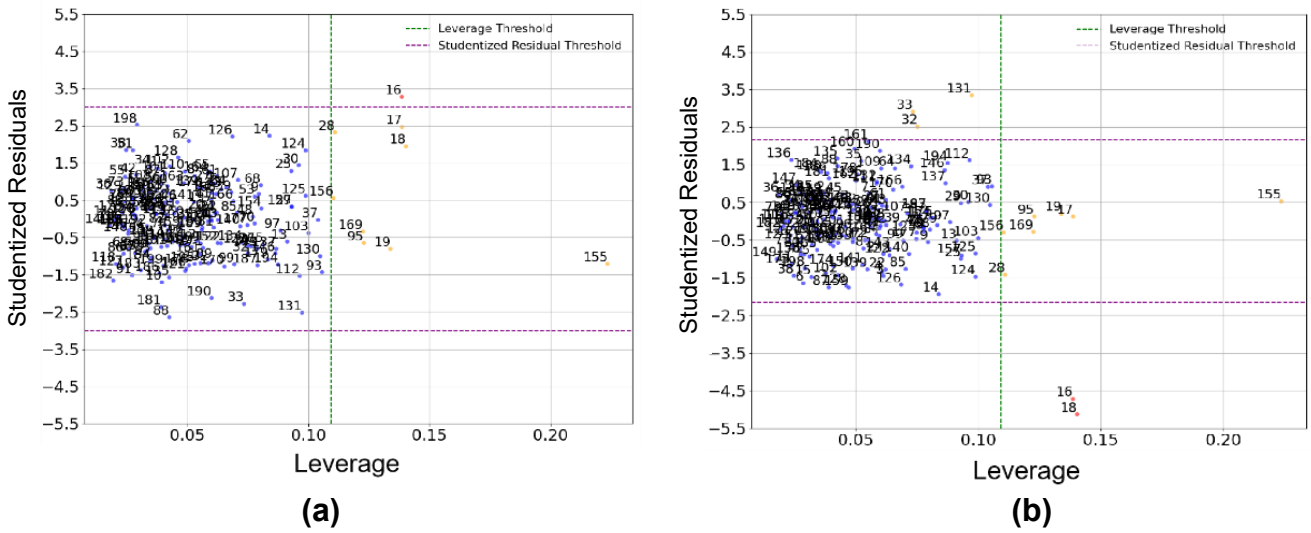

Fig. 3. Leverage-Studentized residuals abnormal sample rejection plot. (a) Abnormal sample rejection of crude protein; (b) Abnormal sample rejection of starch

Table 1. Statistical Data of Measured Results for Crude Protein and Starch Content in Pellet Feed

Category	Number of Anomalous Samples	Range (g/100g)	Mean	SD
Crude Protein	1	7.3889-21.1555	10.1998	2.0215
Starch	2	16.1565-37.2638	3.1613	3.2136

Spectral information division

Sample set partitioning based on joint X-Y distances (SPXY) was used to partition the sample set after rejecting abnormal samples, which integrates the distances between the independent variable X and the dependent variable Y, which can ensure the consistency and balance between the calibration set and the validation set in terms of data distribution and representativeness (Moen *et al*. 2021). In this study, the experimental data after rejecting abnormal samples were divided into correction and prediction sets using the SPXY classification method at a ratio of 3:1.

Preprocessing methods

Due to factors such as instrument performance, environmental conditions during testing, and measurement conditions, directly acquired spectral images often contain some noise. This noise is typically distributed at the baseline and peak signals, making it difficult to identify within the total signal. To mitigate or even eliminate the effect of noise, the main preprocessing methods used in this study included mean centering (MC), standard normal variate (SNV), Savitzky-Golay (SG) convolutional smoothing (with a derivative order of 2 and a smoothing point of 9), and orthogonal signal correction (OSC) for spectral data preprocessing.

Extraction of Effective Wavelengths

Due to the characteristics of full-spectrum data, such as high dimensionality, many bands, large data volume, and redundant information, a significant amount of computation is required when establishing the prediction model. Therefore, to reduce computational demands, the original data must be downscaled. In this study, competitive adaptive reweighted sampling (CARS) (Li *et al.* 2009) and Gradient Boosting (GB) (Bentéjac *et al.* 2021) methods were used to extract the effective wavelengths.

Extraction of Textural Data

Texture features are important visual features in image analysis, reflecting the spatial structure and homogeneity of an image. They not only reveal the macroscopic properties of the sample but also provide insight into its microstructure. The gray-level co-occurrence matrix (GLCM) is the most widely used technique for texture analysis, extracting features by analyzing the spatial relationships of pixel gray values in an image (Jiang *et al*. 2019). Since images captured at different angles and distances can produce varying gray-level co-occurrence matrices, this study sets the distance to 1 and considers four texture features—energy, entropy, homogeneity, and correlation—at four different directions (0, 45, 90, and 135°).

Before extracting texture features, principal component analysis (PCA) was performed on the hyperspectral image data. The texture features of the image were successfully extracted by the GLCM analysis of the first principal component (PC1) score image and explained 95.39% of the variance. Based on this, texture variables were calculated for all samples, and the average texture values in different directions were selected as the texture features for each sample. In the end, four texture features were obtained from each image for subsequent modeling analysis.

Model Development and Evaluation

The support vector regression (SVR) model was used to predict crude protein and starch content in feed pellets. SVR is an application of the Support Vector Machine (SVM), primarily used for reliability analysis and response prediction. The basic idea behind SVR is to map a nonlinear problem to a high-dimensional space using a kernel function, enabling linear regression for optimal learning.

To evaluate the accuracy and predictive ability of the models, the coefficient of determination (R^2) and root mean square error (RMSE) were used. The closer the R^2 is to 1 and the smaller the RMSE, the higher the correlation between the spectral information extracted by the model and the nutrient content, indicating better model performance and stability.

RESULTS AND DISCUSSION

Prediction Models with Full Spectral Range

In this study, four algorithms , namely MC, SNV, SG convolutional smoothing, and OSC were used to process the raw spectra to eliminate the background information interference.

SVR analysis was performed on the raw and preprocessed spectral data to establish a prediction model for crude protein and starch content in pellet feed. As shown in Fig. 4, when raw spectra were used for the determination of crude protein and starch, the R^2p was 0.8318, and the RMSEP was 0.7550. For starch, the R^2p was 0.7317, and the RMSEP was 1.5816. The results indicate that, compared to raw spectra, the prediction performance with SNV preprocessed spectra was better, exhibiting smaller errors, primarily due to the reduction of noise and bias. This suggests that SNV preprocessing reduces light scattering and non-informative variations, allowing the model to better capture key features, thus improving the prediction accuracy of crude protein and starch.

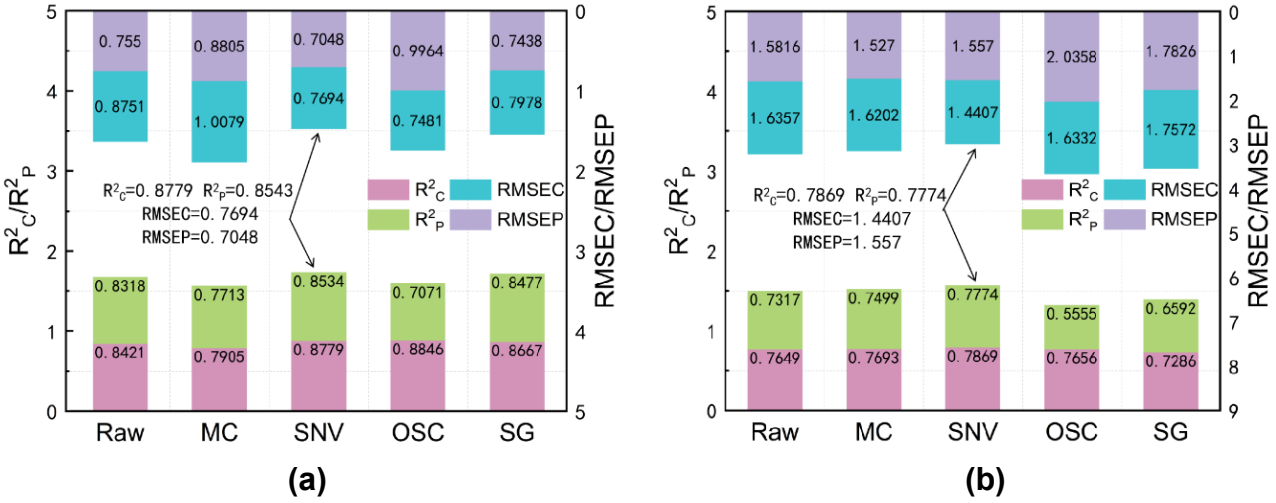

Fig. 4. Performance of full wavelength model based on different pre-processing methods. (a) Crude protein; (b) Starch

Prediction Models with Effective Wavelengths

The first 30 important feature wavelengths extracted by the GB method are shown in Fig. 5. The band corresponding to the wavelength of 1556.1 nm in Fig. 5a was selected as the most important feature for crude protein, while the band corresponding to the wavelength of 1119.6 nm in Fig. 5b was selected as the most important feature for starch. Figures 5c and 5d show the wavelengths corresponding to each feature in the spectral region for crude protein and starch in pelleted feeds, respectively. From Fig. 5c, it can be observed that the characteristic bands selected by crude protein were primarily concentrated from 1100 to 1140 nm and 1450 to 1650 nm. The band at 1450 to 1550 nm is associated with the N-H bending vibration in the protein, while the band at 1600 to 1650 nm is mainly attributed to the C=O stretching vibration in the peptide bond of the protein (Yan 2005).

The effective wavelengths were extracted from the crude protein and starch spectral data using the CARS method, with the Monte Carlo sample size set to 40 and incorporating 10-fold cross-validation. Figure 6a represents the trend of the root mean square error

(RMSE) as a function of the number of samples in the cross-validation. Figure 6b shows the path of the regression coefficients during each sampling, with the thick vertical line indicating the minimum value of RMSECV, which occurs when the number of sampling runs is 35. At this point, the information unrelated to crude protein is excluded, and a total of 44 feature wavelengths that provide the most relevant information are selected. Figure 6c illustrates the corresponding wavelengths for crude protein in pellet feed within the spectral region. The effective wavelengths of the starch content samples, extracted by the CARS method, are shown in Fig. 7, with a total of 44 effective wavelengths selected. As shown in Fig. 7c, the characteristic bands selected for starch are primarily concentrated from 1150 to 1200 nm and 1400 to 1550 nm. The band at 1150 to 1200 nm is associated with the stretching vibration of the starch C-H bond, while the band at 1450 to 1550 nm is mainly related to the -OH stretching vibration (Yan 2005).

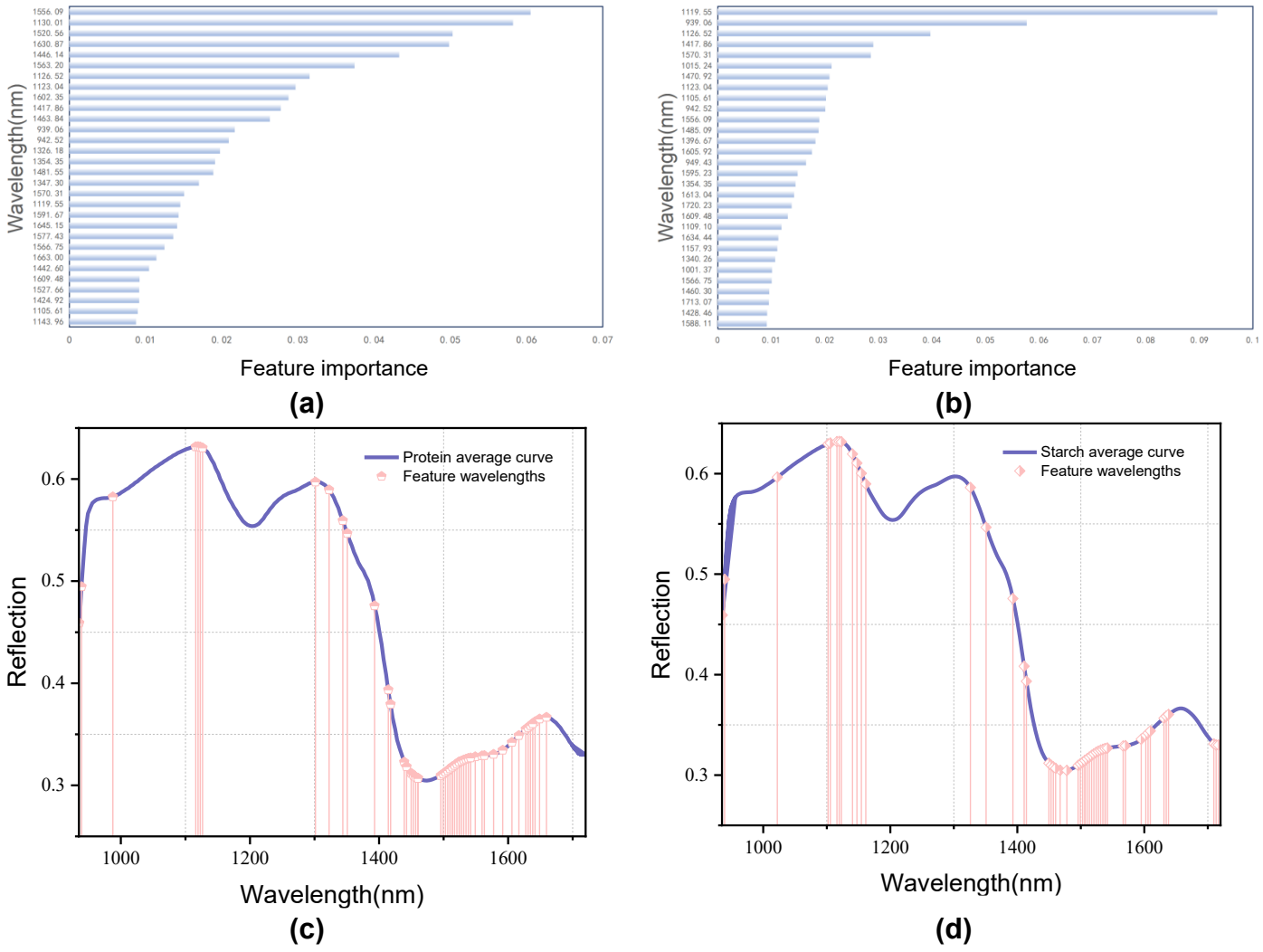

Fig. 5. Results of feature wavelengths extracted by the GB algorithm. (a) Top thirty feature bands of crude protein contribution; (b) Top thirty feature bands of starch contribution; (c) Distribution of crude protein effective wavelengths; (d) Distribution of starch effective wavelengths

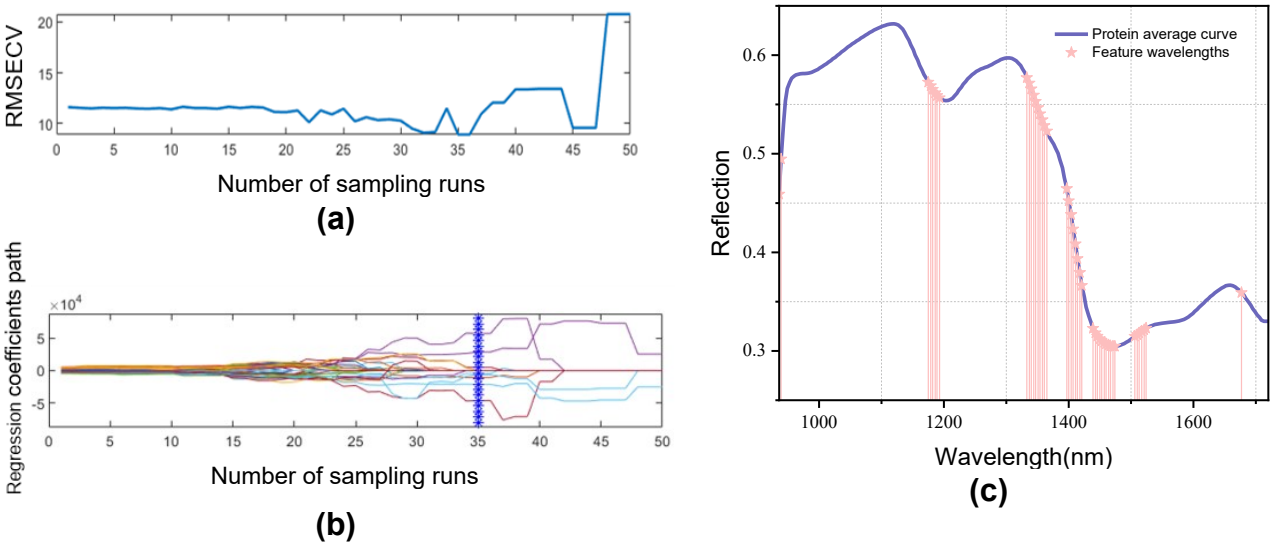

Fig. 6. Result of CARS effective band selection for crude protein. Different color curves represent different variables. (a) Trend of RMSECV with increasing sample size; (b) Trend of extracted variables with increasing sample size; (c) Distribution of effective wavelengths

Table 2 presents the statistical results of the crude protein and starch content predictions, where crude protein and starch were predicted using full spectral variables, as well as spectral variables selected by the CARS method and the GB algorithm, respectively.

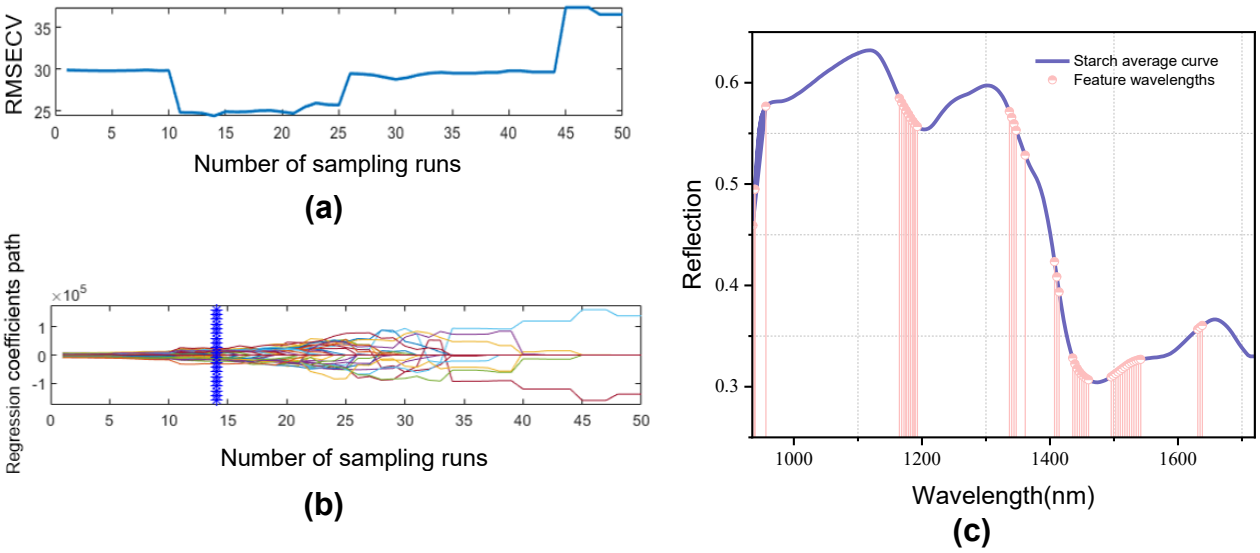

Fig. 7. Result of CARS effective band selection for starch. Different color curves represent different variables. (a) Trend of RMSECV with increasing sample size; (b) Trend of extracted variables with increasing sample size; (c) Distribution of effective wavelengths

For the prediction of crude protein, the full-spectrum method (224 bands) demonstrated good fitting performance on both the calibration and prediction sets, with an R^2c of 0.8779, an R^2p of 0.8534, and RMSEC and RMSEP values of 0.7694 and 0.7048, respectively. The CARS method (44 bands) further improved prediction performance, with an R^2p of 0.8812 and RMSEP reduced to 0.5919. The GB method (30 bands) performed

the best, with an R^2p of 0.8861 and a minimum RMSEP of 0.5845. The above results show that the 30 optimal wavelengths selected using the GB method were information-rich and suitable to effectively replace the full-wavelength method.

Table 2. Performance of the Developed Models Based on the Full Wavelength and Effective Wavelength of Crude Protein and Starch Contents

Category	Model	No. of variables	Extraction method	Calibration set		Prediction set	
				R^2c	RMSEC	R^2p	RMSEP
Protein	SVR	224	Full spectra	0.8779	0.7694	0.8534	0.7048
		44	Cars	0.8733	0.7877	0.8812	0.5919
		30	GB	0.9027	0.6948	0.8861	0.5845
starch	SVR	224	Full spectra	0.7869	1.5570	0.7774	1.4407
		44	Cars	0.7731	1.6830	0.7752	1.4852
		30	GB	0.7327	1.7407	0.6897	1.7108

For the prediction of starch, the prediction performance of all three band selection methods was inferior to that of the crude protein samples. Although the full-spectrum method (224 bands) demonstrated some predictive ability, with an R^2c of 0.7869 and an R^2p of 0.7774, the RMSEC and RMSEP were relatively large, at 1.5570 and 1.4407, respectively, indicating lower model fitting and prediction accuracy. The prediction performance of the CARS method (44 bands) after feature extraction was further degraded, with an R^2p of 0.7752 and an RMSEP of 1.4852, indicating a significant increase in error. The GB method (30 bands) showed the worst prediction performance after feature extraction, with an R^2p of 0.6897 and an RMSEP of 1.7108, resulting in the largest prediction error. Because the prediction model for starch performed poorly under all band selection methods, the CARS method was selected as the preferred method for selecting starch effective wavelengths for subsequent modeling, based on a comprehensive assessment.

Prediction Models Integrated with Spectral and Textural Data

Before fusing the texture data with the spectral data, each region of interest (ROI) image was subjected to PCA to reduce the spectral dimensions. By extracting the first three principal component images (PC1, PC2, and PC3), their cumulative spectral variances were obtained to be 95.39%, 4.16%, and 0.21%, respectively. Therefore, the PC1 image was selected as the best representation of the original sample for subsequent texture information extraction.

Figure 8 illustrates the Pearson correlation between crude protein and starch content and the textural parameters (energy, entropy, homogeneity, and correlation). From the figure, it can be seen that crude protein and starch content had little correlation with the four texture parameters. Among them, entropy showed the greatest correlation with crude protein, followed by correlation. Starch had the greatest correlation with energy, followed by homogeneity. Because the surface texture features of pellet feed samples had little influence on their crude protein and starch contents, though some correlation still was apparent, entropy and correlation were selected as texture features for crude protein. Meanwhile, energy and homogeneity were chosen as texture features for starch. These features were selected to be applied to the subsequent fusion model.

SVR prediction model based on extracted texture features and optimal spectral data

Table 3 presents the performance data of the developed fusion model in predicting crude protein and starch content, showing an improvement in prediction accuracy.

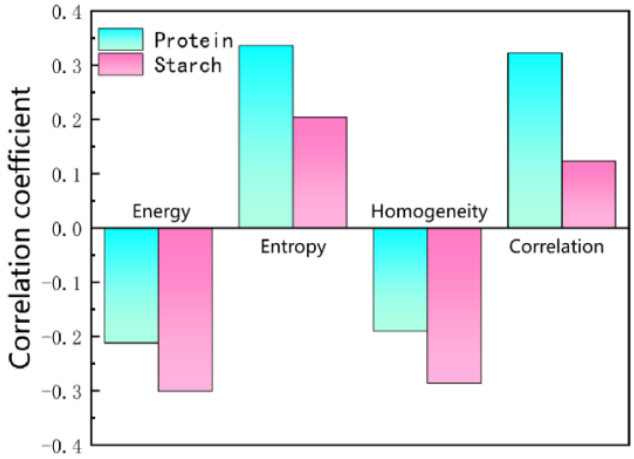

Fig. 8. Correlation between crude protein and starch with texture parameters extracted using GLCM

Table 3. Prediction of Crude Protein and Starch Contents Based on Fused Data

Category	Model	Fusion type	Calibration set		Prediction set	
			R^2c	RMSEC	R^2p	RMSEP
Protein	SVR	GB	0.9027	0.6948	0.8861	0.5845
		GB -ENT	0.8974	0.7153	0.8820	0.5782
		GB- COR	0.9127	0.6513	0.9070	0.5548
		GB-COR-ENT	0.9048	0.6879	0.8169	0.7296
Starch	SVR	CARS	0.7731	1.6830	0.7752	1.4852
		CARS-ENE	0.7654	1.6310	0.7915	1.3970
		CARS-HOM	0.7610	1.6513	0.7906	1.3864
		CARS -ENE-HOM	0.7425	1.7085	0.735	1.5745

For crude protein prediction, the SVR model combining COR parameters (GB-COR-SVR) outperformed the SVR models using spectral data alone or incorporating other texture parameters. Specifically, the GB-COR-SVR model achieved an R^2c of 0.9127, an R^2p of 0.9070 an RMSEC of 0.6513, and an RMSEP of 0.5548. Compared to the model built with the effective wavelengths, the R^2p value was increased by 0.0209, while the RMSEP value decreased by 0.0297. For starch prediction, the CARS-ENE-SVR model performed the best, outperforming models that used spectral data alone or incorporated other texture parameters. This was demonstrated by an R^2c of 0.7654, R^2p of 0.7915, RMSEC of 1.6310, and RMSEP of 1.3970.

In summary, the fusion of texture parameters and spectral features significantly improved the accuracy of predicting crude protein and starch contents, with crude protein predictions being more accurate than starch. However, the model still faces challenges in real-world applications: environmental factors such as light, temperature, and humidity may introduce noise, affecting prediction stability, and the model's generalizability needs further validation, as current samples are mainly from specific regions and materials.

Future research should focus on enhancing data robustness, optimizing real-time predictions, and expanding sample diversity to improve the model's applicability in broader production scenarios.

CONCLUSIONS

1. In order to quickly and accurately detect the crude protein and starch content in alfalfa-potato pomace pellets, this study utilized hyperspectral imaging technology to collect hyperspectral images of the particles in the 900 to 1700 nm wavelength range. Additionally, various spectral preprocessing methods and effective wavelength selection techniques were combined to construct a support vector regression (SVR) model. The results demonstrated that the 30 and 44 effective wavelengths selected by Gradient Boosting (GB) and competitive adaptive reweighted sampling (CARS) showed good validity for predicting crude protein and starch content.
2. To further improve prediction accuracy, this study incorporated texture features based on spectral data. Texture features, including energy, entropy, homogeneity, and correlation, were extracted using the gray-level co-occurrence matrix (GLCM). The modeling analysis of the fused mapping information revealed that the SNV-GB-COR-SVR fusion model was the most effective for predicting crude protein, with an R^2p of 0.907 and an RMSEP of 0.5548. Meanwhile, the SNV-CARS-ENT-SVR fusion model performed best for predicting starch content, with an R^2p of 0.7915 and an RMSEP of 1.3970.

ACKNOWLEDGMENTS

The authors are grateful for the support of the National Natural Science Foundation of China (32360852), National Natural Science Foundation of China (31960365), First Class Disciplines Research Special Project (YLXKZX-NND-046), and Innovation Start-up Support Program for Overseas-educated Scholars in Inner Mongolia (2022).

REFERENCES CITED

Bentéjac, C., Csörgő, A., and Martínez-Muñoz, G. (2021). "A comparative analysis of gradient boosting algorithms," *Artificial Intelligence Review* 54, 1937-1967. DOI: 10.1007/s10462-020-09896-5

Cheng, W., Sun, D. W., Pu, H., Zhang, Q., and Liu, Y. (2016). "Integration of spectral and textural data for enhancing hyperspectral prediction of K value in pork meat," *LWT-Food Science and Technology* 72, 322-329. DOI: 10.1016/j.lwt.2016.05.003

Du, H., Zhang, Y., and Ma, Y. (2024). "Rapid determination of crude protein content in alfalfa based on Fourier transform infrared Spectroscopy," *Foods* 13(14), 2187-2187. DOI: 10.3390/foods13142187

Fu, M., Liu, M., and Niu, Z. (2017). "Inspection method of feed main nutritional components by NIRS and hyperspectral imaging," *Journal of Huazhong Agricultural University* 36(2), 123-129.

Guo, W., Gao, J., Wang, H., Zhang, W., and Li, Y. (2017). "The approaches of reusing potato pulp and its development countermeasures," *Food Research and Development* 38(16), 205-208.

Hadidi, M., Palacios, J. C. O., McClements, D. J., Figueroa, M. A., and Lopez, C. (2023). "Alfalfa as a sustainable source of plant-based food proteins," *Trends in Food Science & Technology* 135, 202-214. DOI: 10.1016/j.tifs.2023.03.023

Huang, J., Qian, M., Jia, N., Zhang, X., and Liu, Y. (2021). "Research progress in the determination of nutrients in feed by spectroscopy," *South China Agricultural Machinery* 52(20), 4-10.

Jiang, H. Z., Yoon, S. C., Zhuang, H., Wang, W., Li, Y. F., and Yang, Y. (2019). "Integration of spectral and textural features of visible and near-infrared hyperspectral imaging for differentiating between normal and white striping broiler breast meat," *Spectrochimica Acta Part A: Molecular & Biomolecular Spectroscopy* 213, 118-126. DOI: 10.1016/j.saa.2019.01.052

Li, H., Liang, Y., Xu, Q., Zhang, J., and Chen, S. (2009). "Key wavelengths screening using competitive adaptive reweighted sampling method for multivariate calibration," *Analytica Chimica Acta* 648(1), 77-84. DOI: 10.1016/j.aca.2009.06.046

Liu, D., Pu, H., Sun, D. W., Zhang, Y., and Zhao, W. (2014). "Combination of spectra and texture data of hyperspectral imaging for prediction of pH in salted meat," *Food Chemistry* 160, 330-337. DOI: 10.1016/j.foodchem.2014.03.096

Moen, J. E., Nilsen, V., Saidi, K. B., Kohmann, E., Devassy, B. M., and George, S. (2021). "Hyperspectral imaging and machine learning for the prediction of SSC in kiwi fruits," *Norsk IKT-konferanse for forskning og utdanning* 1, 86-98.

Rocha, G. C., Duarte, M. E., Kim, S. W., and Silva, L. (2022). "Advances, implications, and limitations of low-crude-protein diets in pig production," *Animals* 12(24), article 3478. DOI: 10.3390/ani12243478

Rukundo, I. R., Danao, M-G. C., MacDonald, J. C., Wehling, R. L., and Weller, C. L. (2021). "Performance of two handheld NIR spectrometers to quantify crude protein of composite animal forage and feedstuff," *AIMS Agriculture and Food* 6(1), 463-477. DOI: 10.3934/AGRFOOD.2021027

Tang, Y., Huang, J., and Wang, R. (2004). "Study on estimating the contents of crude protein and crude starch in rice panicle and paddy by hyperspectral," *Chinese Agricultural Sciences* 2004(09), 1282-1287.

Wang, C., Wang, S., He, X., Zhang, Y., and Sun, L. (2020). "Combination of spectra and texture data of hyperspectral imaging for prediction and visualization of palmitic acid and oleic acid contents in lamb meat," *Meat Science* 169, article 108194. DOI: 10.1016/j.meatsci.2020.108194

Xie, G. (2013). *The Rapid Detection Method and Model Establishment of Dry Matter and Soluble Sugar of Rice and Rape Straw by Near Infrared Reflectance Spectroscopy*, Master's Thesis, Huazhong Agricultural University, Wuhan, China.

Yan, F. (2005). *Basics and Applications of Near-Infrared Spectral Analysis*, China Light Industry Press, Beijing.

Yan, J., Chen, H., and Liu, L. (2019). "Overview of hyperspectral image classification," *Optics and Precision Engineering* 27(3), 680-693. DOI: 10.3788/OPE.20192703.0680

Yang, D., Lu, A., and Wang, J.(2017). "Quantification and visualization of total volatile basic nitrogen content of cooked beef by hyperspectral imaging technique," *Modern Food Science and Technology* 33(9), 257-264.

Yang, X. (2024). *Soil Moisture Content Estimation Model Based on Hyperspectral Image Texture and Spectral Feature Fusion*, Master's Thesis, Northwest A&F University, Xianyang, China.

Yu, Z., Chen, X., Zhang, J., Su, Q., Wang, K., and Liu, W. (2023). "Rapid and non-destructive estimation of moisture content in Caragana Korshinskii pellet feed using hyperspectral imaging," *Sensors* 23(17), article 7592. DOI: 10.3390/s23177592

Zhang, M. (2023). *Research on the Detection and Grading of Silage Corn Feed Quality based on Hyperspectral*, Master's Thesis, Inner Mongolia Agricultural University, Hohhot, China.

Article submitted: April 15, 2025; Peer review completed: September 27, 2025; Revised version received and accepted: September 29, 2025; Published: October 13, 2025.
DOI: 10.15376/biores.20.4.10249-10262